Boundary simulations in realistic wall geometry with the GBS code

Louis Stenger[1], Jochen Hinz[2], Annalisa Buffa[2] & Paolo Ricci[1]

[1] École Polytechnique Fédérale de Lausanne (EPFL), Swiss Plasma Center (SPC), CH-1015 Lausanne, Switzerland
[2] Institute of Mathematics, École Polytechnique Fédérale de Lausanne (EPFL), CH-1015 Lausanne, Switzerland

TSVV3, 2024-10-02

https://infoscience.epfl.ch/handle/20.500.14299/241070

Abstract

- Increased divertor closure has been observed to induce higher divertor neutral pressures thereby facilitating access to detached regimes e.g. in TCV [1] and numerical studies e.g. SOLPS-ITER [2].
- A numerical scheme incorporating a flexible first wall geometry is implemented in the GBS code for boundary plasma simulation.
- The implementation, targeting the plasma module of GBS, is performed using single-block structured curvilinear finite differences.
- Relevant plasma profiles can be retrieved using a synthetic test case. Simulations of a reduced size TCV domain in SILO baffled configuration are presented.

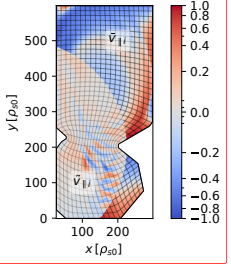

Modeling with GBS

The Global Braginskii Solver (GBS) [3, 4]

- Evolves the two-fluid (electron-ion) drift-reduced Braginskii equations including electromagnetic perturbations in 3D
- Provides a kinetic neutral solver based on the method of characteristics
- Supports arbitrary magnetic geometries
- Performs spatial discretization with 4th order central finite differences
- Advances time with fixed/variables explicit RK time-steppers
- Solves electrostatic (Poisson) and electromagnetic (Ampère) perturbations iteratively using PETSc' GMRES
- Scales to more than 10^4 CPUs (pure MPI), has been GPU ported.

In particular, spatial discretization

- relies on staggered Cartesian grids,
- splits even (e.g. density) and odd (e.g. velocities) moments on separate grids to avoid odd-even decoupling.

The code is extended to support *curvilinear finite differences* allowing a more general class of grids,

- Discretize and evolve GBS equations in a "computational space" $\boldsymbol{\xi} \in \hat{\Omega} = (0,1)^2$.
- Find a map $\mathbf{X}(\boldsymbol{\xi}) = (x, y) : \hat{\Omega} \mapsto \Omega \subset \mathbb{R}^2$ that yields the desired first wall geometry $\partial\Omega$. (x, y) denote the radial R, resp. vertical Z, directions.

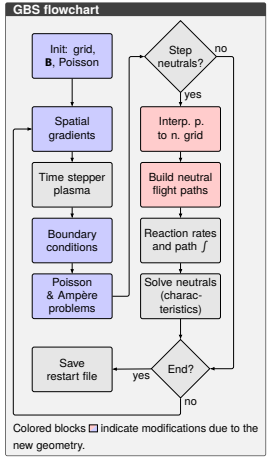

Spatial operators are expanded in terms of $\boldsymbol{\xi}$ coordinates, e.g.

$$C(f) = \partial_y f = \partial_y \xi^i \partial_{\xi^i} f,$$
$$\partial_s f = \hat{\mathbf{n}} \cdot \nabla f = \pm\sqrt{g_{kk}} g^{hj} \partial_{\xi^j} f.$$

Synthetic benchmarks

Verify RHS implementation on a grid with rectangular boundary. Let $\mathbf{X}_0(\boldsymbol{\xi}) = [L_x, L_y]\boldsymbol{\xi}$ the original Cartesian map.

$$\mathbf{X}(\boldsymbol{\xi}) = \mathbf{X}_0(\boldsymbol{\xi}) - A_s \frac{\delta}{\delta_s} \exp\left(-\frac{(\delta-\delta_s)^2}{2w_s^2}\right)\begin{bmatrix}\sin(\theta)\\ -\cos(\theta)\end{bmatrix},$$

where $L_x = 300$, $L_y = 400$, $A_s = 30$, $\delta_s = 75$, $w_s = 20$, and δ and θ defined as

$$\delta(\boldsymbol{\xi}) = |\mathbf{X}_0(\boldsymbol{\xi}) - \mathbf{X}_0(0.5)|,$$
$$\theta(\boldsymbol{\xi}) = \operatorname{atan2}(\mathbf{X}_0(\boldsymbol{\xi}) - \mathbf{X}_0(0.5)).$$

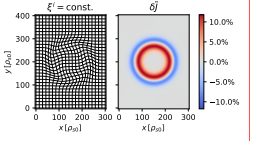

Figure 1: The resulting grid and relative difference in Jacobian $\delta\tilde{J}$ indicates the volumetric contraction/expansion of grid cells.

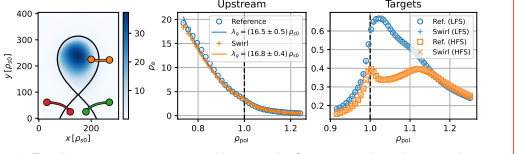

Figure 2: Excellent agreement is recovered between the Cartesian and curvilinear implementations. Here, electron pressure profiles are compared at the outboard midplane, high- and low-field side targets.

Baffled TCV configurations

The "Short In Long Out" (SILO) baffled TCV configuration with reduced toroidal magnetic field ($B_0 = 0.9$ T) is considered. The domain is scaled to 1/3 of its original size to lower computational cost. Boundary definition is provided as an ordered point set P. Grid generation employs spline-based meshing techniques based on [5, 6],

1. Four $C^2(\mathbb{R}^2)$ splines are fitted to P defining $\partial\Omega$,
2. A spline map is computed by an elliptic solver & optimized for cell size homogeneity,
3. Sample the resulting map (and derivatives) on two staggered structured Cartesian meshes in $\hat{\Omega}$.

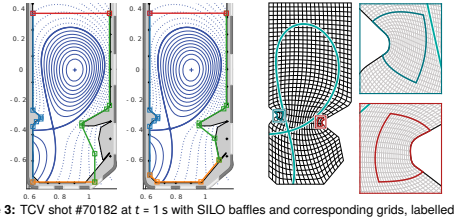

Figure 3: TCV shot #70182 at $t = 1$ s with SILO baffles and corresponding grids, labelled **R**ough (left) and **A**ccurate (right).

Effects of baffling

A set of 7 simulations are performed and labelled `<grid><equil.><suffix>`, e.g. "CXb", where `grid`=`[CRA]` (**C**artesian, also see Fig 3), `<equil.>`=`[XL]` the magnetic equilibrium (**X**21 configuration #78172 [7] and **L**ong-leg configuration #76142) and `<suffix>` to differentiate similar configurations. The following observations hold,

- Taking into account reduced TCV size, the LCFS and baffle tip are ~ 2 cm apart,
- The baffles shadow the plasma in the divertor, resulting in the shrinking of radial profiles,
- Enhanced flows towards the baffle surface and high electrostatic potential are observed resulting from Bohm boundary conditions $v_{\parallel e}^{se} = c_s$, $\phi^{se} = 3T_e$,
- The larger flows to the baffle could explain the decrease in turbulence intensity near the baffle surface, the $E\times B$ shear near the baffle tips is unaffected by the Bohm boundary conditions.

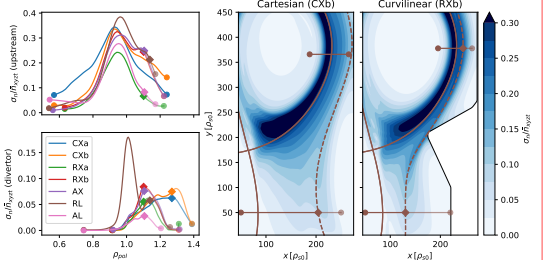

Figure 4: Normalized density fluctuations $\sigma_n/\bar{n}_{xyzt}$ across the simulation set. The dashed line / ◆ symbol indicates the last flux surface connecting both targets.

Future work

The first GBS simulations including plasma dynamics in realistic wall geometry have been performed for a baffled TCV configuration. Future work will focus on

- Enabling curvilinear geometry support for neutrals,
- Optimizing the spline map for other properties than homogeneity: local alignment to flux surfaces, contraction/expansion depending on magnetic geometry region,
- Considering alternative approaches to handle geometries that do not map well to unit square, e.g., immersed boundary conditions [8], multi-block meshes.

Bibliography

[1] O. Février et al. In: *Nucl. Mater. Energy* 27 (2021). DOI: 10.1016/j.nme.2021.100977.
[2] G. Sun et al. In: *Nucl. Fusion* 63.9 (2023). DOI: 10.1088/1741-4326/ace45f.
[3] P. Ricci et al. In: *Plasma Phys. Controlled Fusion* 54.12 (2012). DOI: 10.1088/0741-3335/54/12/124047.
[4] M. Giacomin et al. In: *J. Comput. Phys.* 463 (2022). DOI: 10.1016/j.jcp.2022.111294.
[5] J. Hinz et al. In: *Comput. Aided Geom. Des.* 65 (2018). DOI: 10.1016/j.cagd.2018.03.023.
[6] J. Hinz et al. 2023. DOI: 10.48550/arXiv.2307.06265. arXiv: 2307.06265 [cs, math].
[7] D. S. Oliveira et al. In: *Nucl. Fusion* 62.9 (2022). DOI: 10.1088/1741-4326/ac4cde.
[8] T. Body et al. In: *Contrib. Plasma Phys.* 60.5-6 (2020). DOI: 10.1002/ctpp.201900139.

Louis Stenger, Swiss Plasma Center, EPFL

Swiss Plasma Center

EUROfusion

This work has been carried out within the framework of the EUROfusion Consortium, funded by the European Union via the Euratom Research and Training Programme (Grant Agreement No 101052200 — EUROfusion). Views and opinions expressed are however those of the author(s) only and do not necessarily reflect those of the European Union or the European Commission. Neither the European Union nor the European Commission can be held responsible for them.

1. Four $C^2(\mathbb{R}^2)$ splines are fitted to P defining $\partial\Omega$,
2. A spline map is computed by an elliptic solver & optimized for cell size homogeneity,
3. Sample the resulting map (and derivatives) on two staggered structured Cartesian meshes in $\hat{\Omega}$.

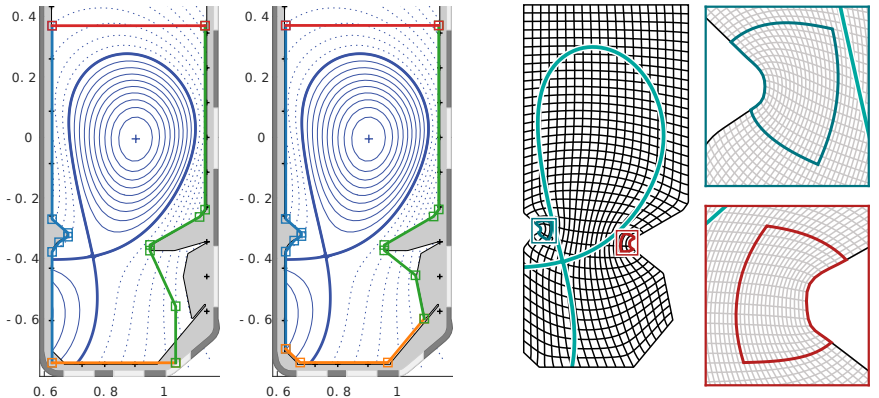

Figure 3: TCV shot #70182 at t = 1 s with SILO baffles and corresponding grids, labelled **R**ough (left) and **A**ccurate (right).

Use curvilinear coordinates

Find transformation (R, Z) as functions of (ξ, χ)

Computational coordinates in unit square: $(\xi, \chi) \in (0,1)^2$

Discretization of (ξ, χ) is still structured / Cartesian

Operators expanded in terms of metric coefficients of the transformation

Spatial operators are expanded in terms of $\boldsymbol{\xi}$ coordinates, e.g.

$$C(f) = \partial_y f = \partial_y \xi^i \partial_{\xi^i} f,$$

$$\partial_s f = \hat{\mathbf{n}} \cdot \boldsymbol{\nabla} f = \pm\sqrt{g_{kk}}\, g^{kj} \partial_{\xi^j} f.$$

Coordinate map can be defined analytically

Good comparison between reference version and curvilinear version when keeping a rectangular wall geometry (expect same profiles)

(also verified through unit tests)

Synthetic benchmarks

Verify RHS implementation on a grid with rectangular boundary. Let $\mathbf{X}_0(\boldsymbol{\xi}) = [L_x, L_y]\boldsymbol{\xi}$ the original Cartesian map.

$$\mathbf{X}(\boldsymbol{\xi}) = \mathbf{X}_0(\boldsymbol{\xi}) - A_s \frac{\delta}{\delta_s} \exp\left(-\frac{(\delta - \delta_s)^2}{2w_s^2}\right) \begin{bmatrix} \sin(\theta) \\ -\cos(\theta) \end{bmatrix},$$

where $L_x = 300$, $L_y = 400$, $A_s = 30$, $\delta_s = 75$, $w_s = 20$, and δ and θ defined as

$$\delta(\boldsymbol{\xi}) = |\mathbf{X}_0(\boldsymbol{\xi}) - \mathbf{X}_0(0.5)|,$$
$$\theta(\boldsymbol{\xi}) = \operatorname{atan2}(\mathbf{X}_0(\boldsymbol{\xi}) - \mathbf{X}_0(0.5)).$$

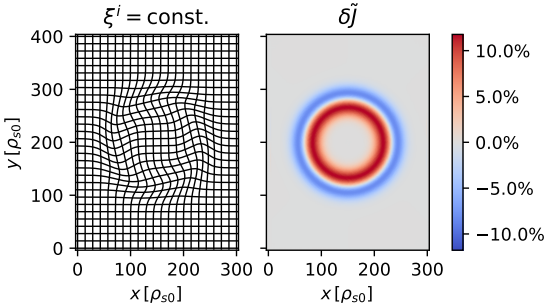

Figure 1: The resulting grid and relative difference in Jacobian $\delta\tilde{J}$ indicates the volumetric contraction/expansion of grid cells.

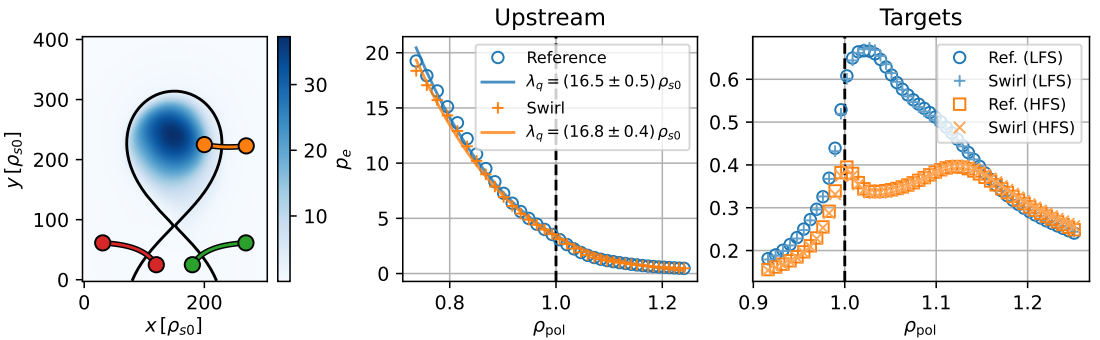

Figure 2: Excellent agreement is recovered between the Cartesian and curvilinear implementations. Here, electron pressure profiles are compared at the outboard midplane, high- and low-field side targets.

Two SILO-baffled 1/3rd TCV curvilinear grid configurations

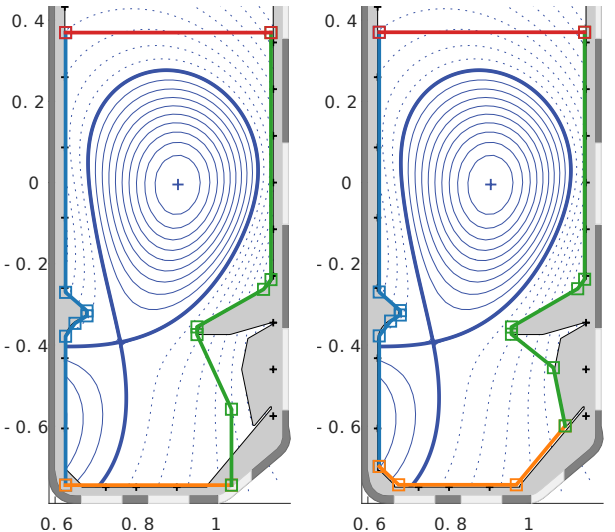

Two magnetic configurations: X21 and “long leg” X-point (#76142).

Runs (electrostatic).

- 4 curvilinear configurations
- 2 comparison domains in reference Cart. GBS

Louis Stenger, Swiss Plasma Center, EPFL

Overall observations (qualitative)

- In general, turbulence above LFS baffle seems slightly weaker than w/o baffle
- Electrostatic potential rises at baffle tip (φ = ΛTe). Does a barrier form? ExB shear (causing lower turbulence levels) ?
- Parallel flows in presence of baffles?

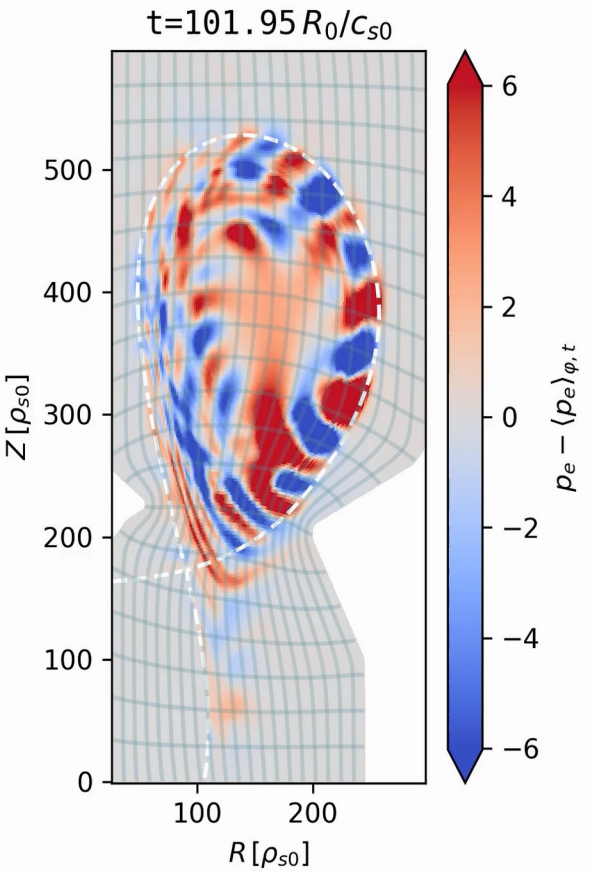

In general, curvilinear sims have slightly lower turbulence levels at outer midplane (LHS, above baffle)

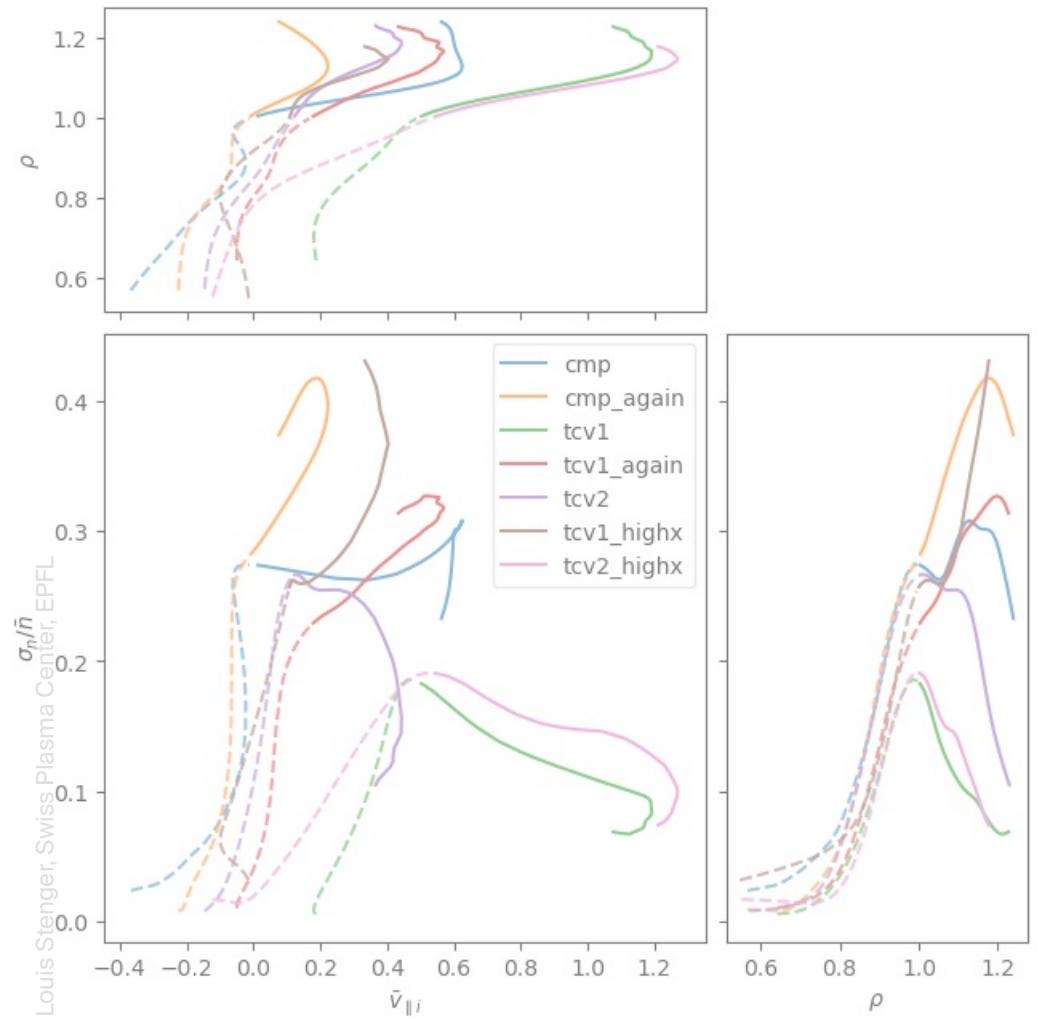

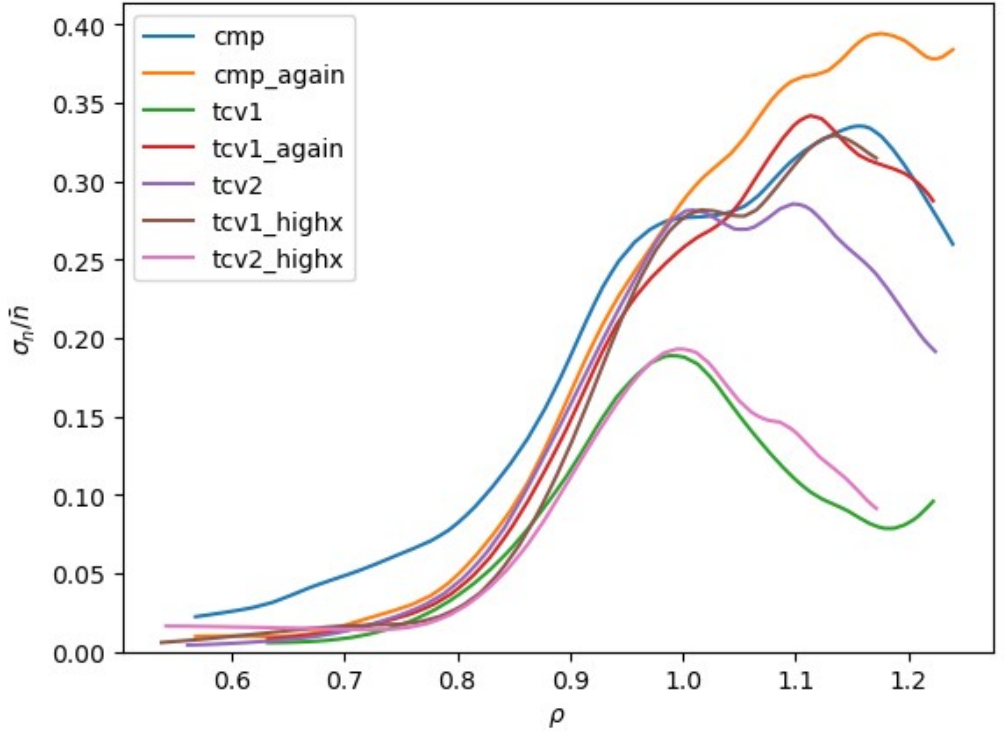

In general, curvilinear sims have slightly lower turbulence levels at outer midplane (LHS, above baffle)

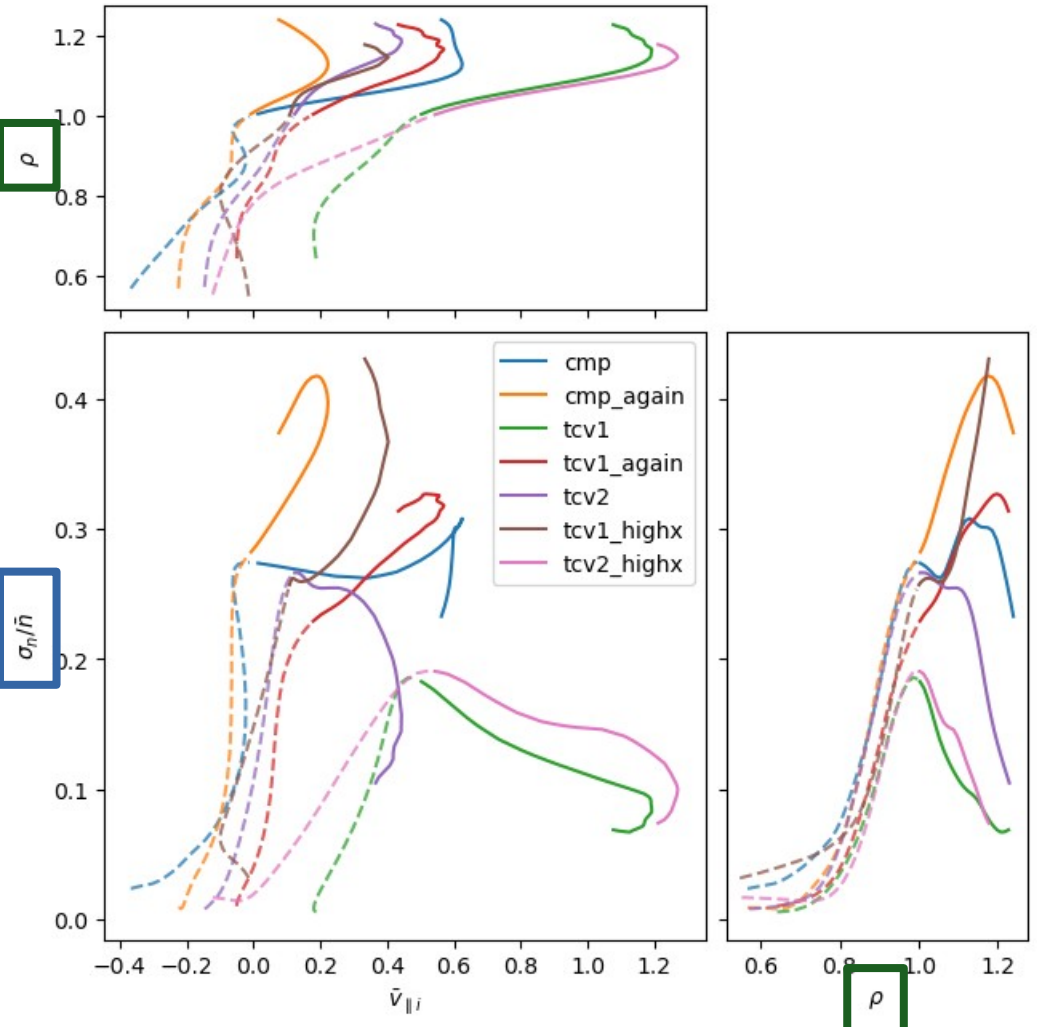

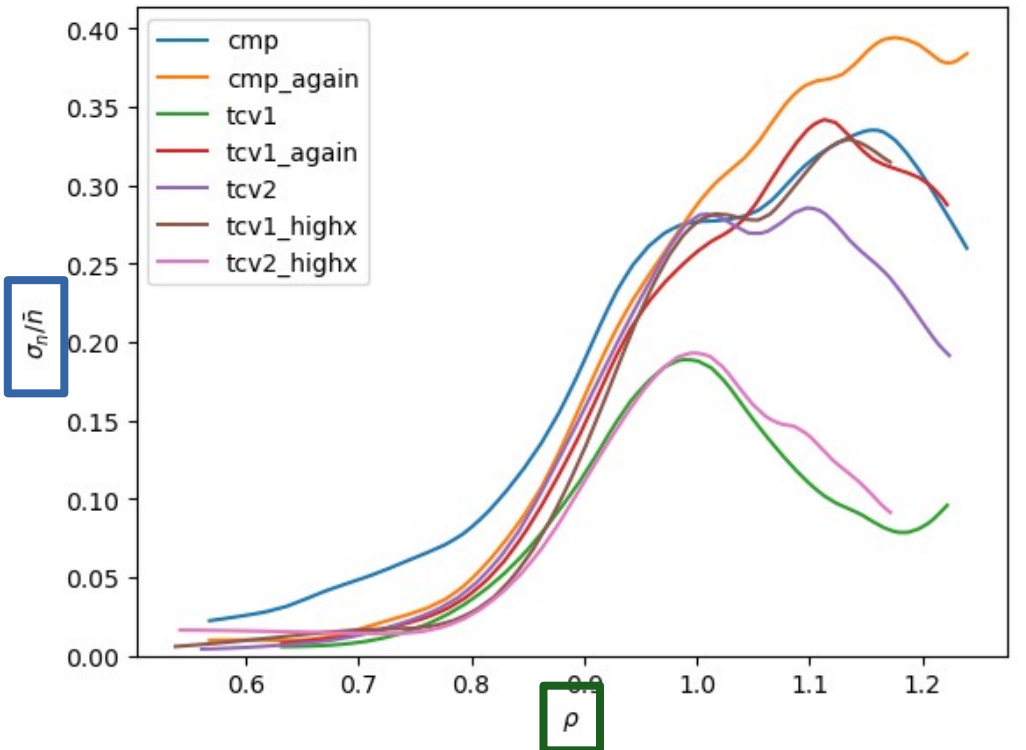

(Electrostatic potential does shift, but ExB shear doesn't increase significantly in baffled case)

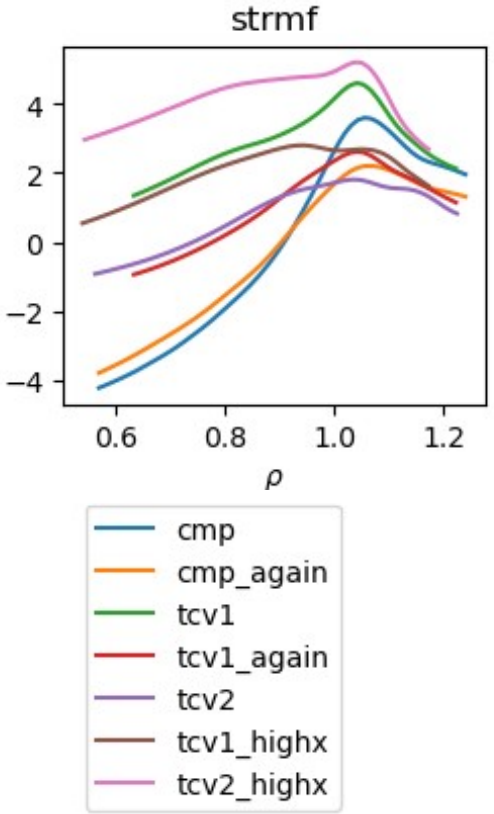

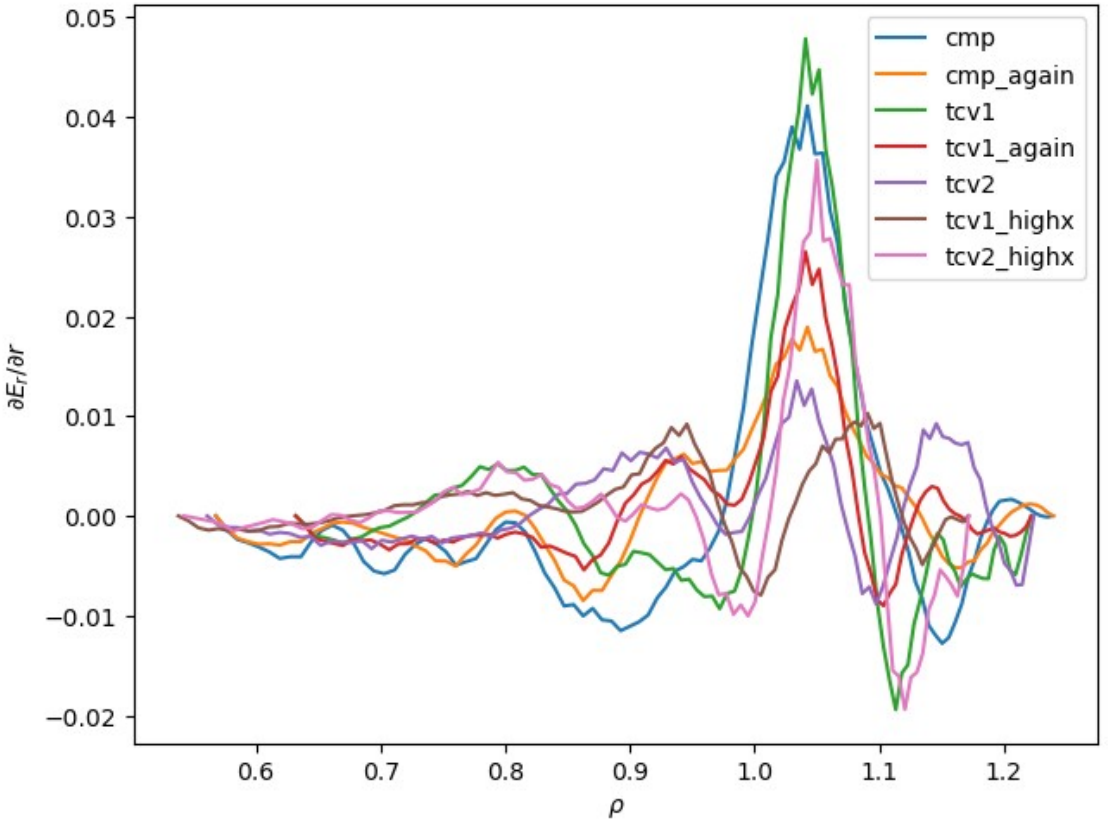

Normalized fluctuations levels drop when reaching the “first wall flux surface” ◆